THE JOURNAL OF PHYSICAL CHEMISTRY B LETTERS

2005, *109,* 19056−19059
Published on Web 09/23/2005

Solid State Synthesis of Tungsten Carbide Nanorods and Nanoplatelets by a Single-Step Pyrolysis

Sangaraju Shanmugam, David S. Jacob, and Aharon Gedanken*

Department of Chemistry and Kanbar Laboratory for Nanomaterials at the Bar-Ilan University Center for Advanced Materials and Nanotechnology, Bar-Ilan University, Ramat-Gan 52900, Israel

Received: July 20, 2005; In Final Form: September 12, 2005

We report a simple and efficient single-step synthesis of tungsten carbide nanorods and nanoplatelets by direct pyrolysis of a hybrid composite material of 12-tungstophosphoric acid and hexadecyltrimethylammonium bromide in a closed Swagelok cell at 1000 °C. The product was characterized by XRD, TGA, SEM, TEM, XPS, and CV. The diameter of the nanorods is 30−50 nm, and the length varies from 200 to 500 nm. The size of the platelets is around 55 nm. The WC exhibits an interesting structural surface with kinks, steps, and terraces which is evidenced by HRTEM studies.

Introduction

Transition metal carbides in general, tungsten carbide in particular, find potential applications due to their special properties, such as high melting point, superior hardness, low friction coefficient, high oxidation resistance, and good electrical conductivity.[1,2] Arie et al. prepared a WC nanoneedle on a tungsten tip by catalytic deposition. The product tested as a scanning tunneling microscope tip.[3] WC was shown to have platinum-like behavior for the chemisorption of hydrogen and oxygen, its applicability as an alternative electrocatalyst of Pt. The early studies showed that this combination of an early transition metal with carbon yielded materials with attractive catalytic activity, stability, selectivity, and resistance to poisoning.[4−9] Recently, there have been several reports on WC as a non-noble metal electrocatalyst in the polymer electrolyte fuel cell (PEFC).[10−12] The most important tungsten carbides are WC and W_2C. W_2C is thermodynamically unstable at low temperatures, while WC is a stable compound. Zellner et al. recently examined the electrochemical stability of WC and W_2C in acidic solutions and found that WC is stable.[13]

There are several routes to prepare tungsten carbide, including direct carburization of tungsten powder, solid state metathesis, reduction−carburization, mechanical milling, and polymeric precursor routes using metal alkoxides.[14−18] WC production generally proceeds as a two-step process. First, the oxide is reduced to a high purity tungsten in a hydrogen atmosphere. The tungsten metal is then mixed with the required amount of carbon and reacts at a temperature of 1400−1600 °C to produce tungsten carbide.[19−21] Herein, we describe a novel and efficient single-step direct pyrolysis of a composite hybrid of 12-phosphotungstic acid ($H_3PW_{12}O_{40}$, PW) and hexadecyltrimethylammonium bromide ($C_{16}H_{33}N(CH_3)_3Br$, CTAB) in a specially designed Swagelok union, which resulted in WC nanorods and nanoplates with quantitative yields.

* Corresponding author. E-mail: gedanken@mail.biu.ac.il.

Experimental Section

The composite hybrid was prepared by the reaction of 12-phosphotungstic acid and hexadecyltrimethylammonium bromide. Elemental and thermogravimetric analysis revealed that the molar ratio of PW to CTAB in the product was 1:3. The hybrid composite was synthesized by dissolving CTAB in distilled water, and this solution was added slowly to the PW solution by vigorous stirring. The molar ratio of PW and CTAB was kept at 1:3. The white precipitate was filtered and dried at room temperature. From the C, H, N analysis, the formula of as-synthesized product was found to be $[C_{21.95}H_{41.19}N_{1.33}]_3$-$PW_{12}O_{40}$.

The synthesis of WC was carried out by using a Swagelok cell, which was assembled from stainless steel Swagelok parts. A $^3/_4$ in. union part was plugged from both sides by standard caps. For this synthesis, 0.5 g of a composite hybrid of 12-phosphotungstic acid ($H_3PW_{12}O_{40}$, PW) and hexadecyltrimethylammonium bromide ($C_{16}H_{33}N(CH_3)_3Br$, CTAB) was introduced into the cell at room temperature under atmospheric conditions. The filled cell was closed tightly with the other plug and then placed inside an iron pipe at the center of the furnace. The temperature was raised at a heating rate of 40 °C/min. The closed vessel cell was heated at 1000 °C for 10 h. The reaction took place at an autogenic pressure of the precursor. The closed vessel cell (Swagelok) heated at 1000 °C was gradually cooled to room temperature and opened with the release of a little pressure, and 0.325 g of black powder was obtained. The total yield of the obtained material was 65% (relative to the starting material). The final black product was treated with HCl 35% and analyzed by elemental (C, H, N) analysis. The content of the carbon was found to be 6.14 wt %. Energy dispersive X-ray analysis of the sample showed a W to C ratio of 1:1.

Results and Discussion

The phase purity of the product was examined by X-ray diffraction (XRD) using a Bruker AXSD* advanced powder

10.1021/jp0540003 CCC: $30.25 © 2005 American Chemical Society

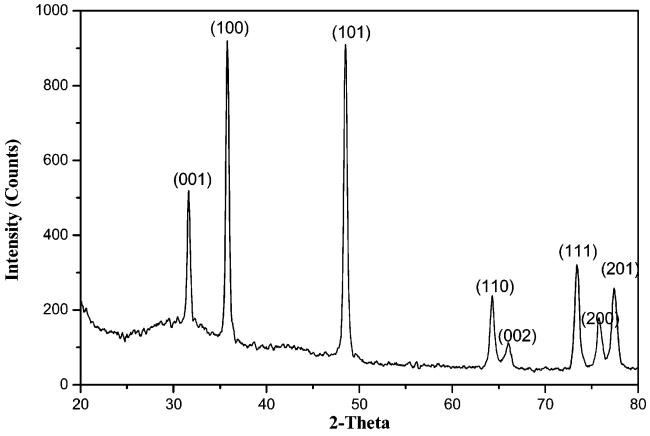

Figure 1. XRD pattern of WC product obtained at 1000 °C for 10 h.

X-ray diffraction using Cu Kα radiation at 40 kV and 45 mV. Figure 1 shows the XRD pattern of the product, and it can readily be indexed to a hexagonal WC with [space group *P*6*m*2 (187)] lattice constants of $a = 2.90$ Å and $c = 2.88$ Å, which match with the literature values (JCPDS 00-051-0939). The morphology of the product was studied with transmission electron microscopy (TEM) on a JEOL-TEM 100 SX microscope. The scanning electron microscopy (SEM) image shows the presence of nanorods and platelets (Figure 2a). The low magnification TEM image of the product consists mainly of rods and platelets (Figure 2b,c). The diameters of the WC rods are 30−50 nm with varying lengths of 600−1000 nm, and the sizes of the platelets are around 55 nm. The high resolution TEM (JEOL 3010 operated at 200 kV) micrographs clearly indicate that the rod is highly crystalline in nature, which is shown in Figure 2d. From the high resolution TEM (HRTEM) studies, it is evident that the growth of the nanorod is mainly along the (001) direction, while the platelets are grown in the direction of the (100) plane

The high resolution TEM image of Figure 2c is presented in Figure 3. It illustrates that the platelet consists of surface features such as steps, kinks, and terraces. Figure 3a shows the lattice fringes with a *d* spacing of 0.252 nm, which closely matches the (100) plane of hexagonal WC. The fast Fourier transform (FFT) pattern of the flat surface of the platelet is consistent with the *d* values observed experimentally. The platelet also contains a grain boundary (001)/(101) which is shown in Figure 3b.

Figure 4a shows the 4f electron photoelectron emission spectra of WC. It exhibits the W 4f5/2 and W 4f7/2 peaks at binding energies of 34.40 and 32.28 eV, respectively, which correspond to the carbidic-modified W. It also demonstrates the oxygen-modified W on the particle's surface at 36.2 and 38.17

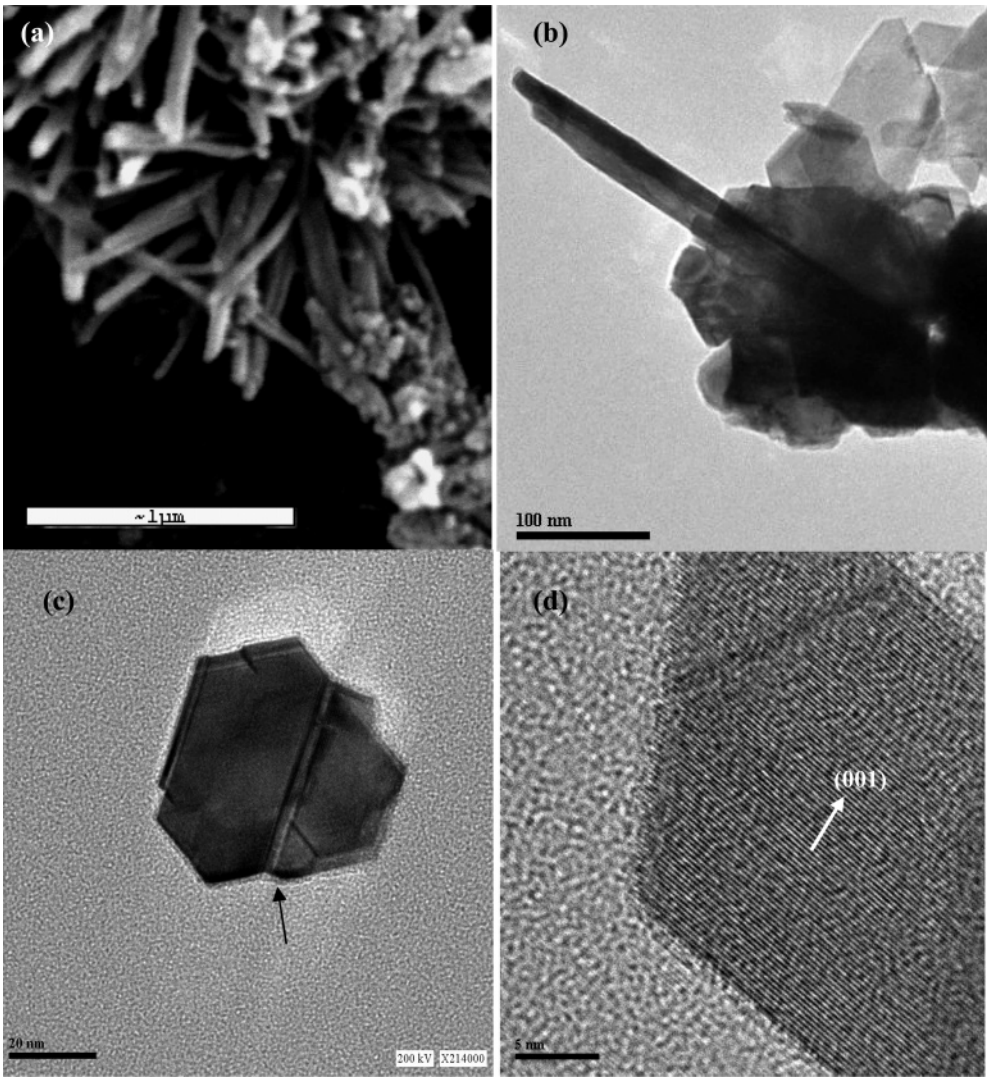

Figure 2. (a) SEM image of WC nanostructures. (b) TEM image showing the coexistence of WC nanorods and nanoplatelets. (c) TEM image of an individual nanoplatelet. (d) HRTEM image of an individual nanorod, with the arrow showing lattice fringes of the WC(001) plane.

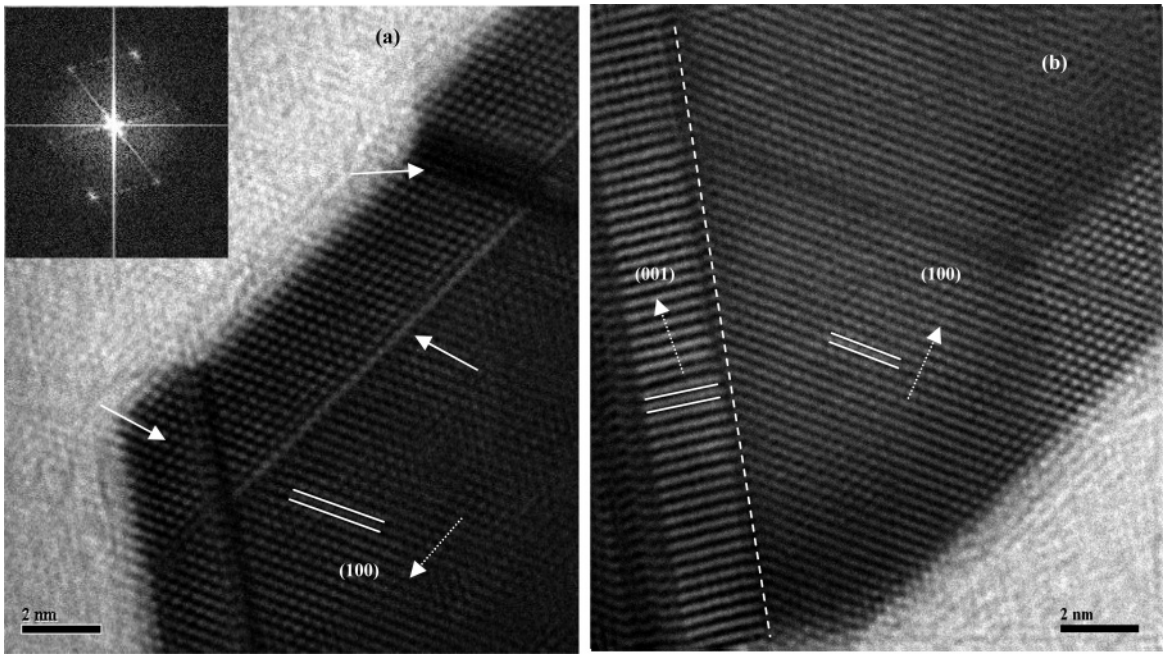

Figure 3. High resolution electron micrographs of the WC platelet shown in Figure 2c. (a) TEM image showing steps, kinks, and terraces. The lattice fringes correspond to the (100) lattice plane of WC. The inset shows a fast Fourier transform (FFT) pattern of the flat surface. (b) HRTEM image showing grain boundary (001)/(100) planes marked with dotted lines. The lattice fringes correspond to the (001) and (100) planes of WC.

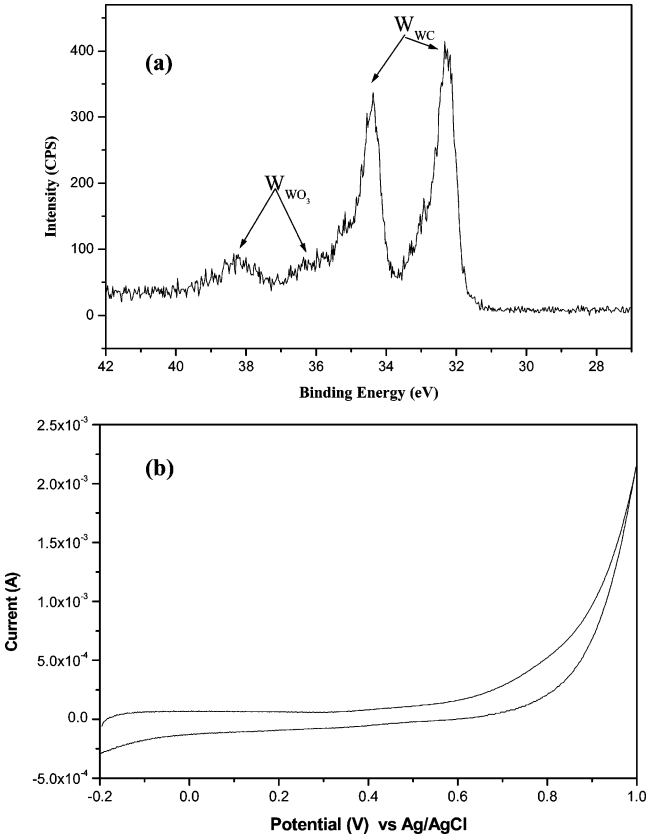

Figure 4. (a) X-ray photoemission spectra of the core electron binding energy of W 4f of WC and (b) cyclic voltammogram of WC in 0.5 M sulfuric acid. Scan rate: 25 mV S^{-1}.

eV. The stoichiometric WC reacted strongly with atmospheric oxygen to passivate the surface.[21] X-ray photoelectron spectroscopy (XPS) showed that the proposition of W^0 to W^{6+} is very small, indicating that the surface is not oxidized. XPS also determined the free carbon contamination of the carbide surface. Two types of carbon peaks were detected at binding energies of 283.3 eV (carbidic) and 284.8 eV (graphitic). The value of the carbidic binding energy is in good agreement with previous data.[22] The energy dispersive X-ray (EDX) and elemental analysis also showed an excess of free carbon (0.14%) on the WC surface. The electrochemical stability of WC was measured in 0.5 M H_2SO_4 using a WC-coated glassy carbon (GC) electrode employed as a working electrode. Figure 4b shows the cyclic voltammogram of WC after the steady state condition. The voltammogram showed a large current increase above 0.6 V, indicating the oxidation of WC. In the reverse scan, there was a cathode current due to the reduction of the oxidized species during the anodic scan.

To determine the effect of temperature on the formation of WC, we performed several experiments at different temperatures in the 800−1000 °C range. It is evident from the XRD analysis that WO_2 is the predominant product at 800 °C, and a mixture of W, W_2C, and WC was observed at 900 °C. When the same reaction was carried out at 1000 °C, but at shorter times, 3 and 6 h, a mixture of WC and W_2C was obtained (SI). Thus, the formation of WC as the sole product in a 10 h reaction at 1000 °C can be explained as follows: First, the precursor is converted to WO_2 and free carbon at low temperatures (800 °C); the free carbon reduces the WO_2 to metallic W at 900 °C. The produced W can further react with carbon, giving rise to tungsten carbide (1000 °C). We have also carried out similar experiments in order to understand the formation of WC by direct pyrolysis of the precursor by varying the anion and cation. We obtained entirely different results. When the anion is changed from heteropolyanion $(PW_{12}O_{40})^{3-}$ to isopolyainon $(W_{10}O_{32})^{4-}$ with the same cation, CTAB, we find open shallow tubes. Early results point out to the formation of carbon nanotubes and W nanoparticles. The formation of WC by the direct pyrolysis of a single precursor is a potential route for the production of WC in large scale.

Conclusions

In conclusion, we have demonstrated the synthesis of single phase WC nanorods and nanoplatelets by a simple and efficient

single-step direct pyrolysis of a hybrid composite material of 12-tungstophosphoric acid and hexadecyltrimethylammonium bromide at relatively low temperatures. The WC nanoplatelets exhibited interesting surface features, which can be exploited in catalysis. The adopted method is not only applicable for tungsten-based polyoxometalates, but it can also be extended to other metals. The method presented here can be easily upscaled to produce WC nanorods in large quantities.

Acknowledgment. The authors thank Dr. Yudith Grinblat and Dr. Y. Gofer for the TEM and XPS analysis. S.S. is thankful to the European community for his postdoctoral fellowship.

Supporting Information Available: XRD patterns of products obtained at 1000 °C for 3 and 6 h and EDX analysis of WC. This material is available free of charge via the Internet at http://pubs.acs.org.

References and Notes

(1) Kosolapva, T. Ya. *Carbides Properties, Production, and Application*; Plenum Press: New York, 1971.

(2) Schwartzkopf, P.; Kieffier, R. *Refractory Hard metals—Borides, Carbides, Nitrides, Silicides*; The MacMillan Company: New York, 1953.

(3) Arie, T.; Akita, S.; Nakayama, Y. *J. Phys. D: Appl. Phys*. **1998**, *31*, L49.

(4) Levy, R.; Boudardt, M. *Science* **1973**, *181*, 547.

(5) Xiao, T.; Hanif, A.; York, E. P. A.; Sloan, J.; Green, H. L. M. *Phys Chem. Chem. Phys.* **2002**, *4*, 3522.

(6) Bendelt, L. H.; Cuthill, J. R.; Mealister, N.; Erickson, N. E. *Science* **1974**, *184*, 563.

(7) Noston, J. E.; Laramore, G. E.; Park, R. L. *Science* **1974**, *185*, 285.

(8) Binder, H.; Kohling, A.; Kuhn, W.; Sandstede, G. *Angew. Chem., Int. Ed.* **1969**, *8*, 757.

(9) Bohm, H. *Electrochim. Acta.* **1970**, *15*, 1273.

(10) Ross, P. N.; Stonehart, P., Jr. *J. Catal*. **1977**, *48*, 42.

(11) Cote, R.; Lalande, G.; Faubert, G.; Guay, D.; Dodelet, J. P.; Denes, G. *J. New Mater. Electrochem. Syst.* **1998**, *1*, 7.

(12) Burstein, G. T.; Mclntyne, D. R.; Vossen, A. *Electrochem. Solid-State Lett.* **2002**, *5*, A80.

(13) Zellner, M. G.; Chen, J. G. *Catal. Today* **2005**, *99*, 299.

(14) Ribeiro, F. H.; Dalla Betta, R. A.; Guskey, G. Y.; Boudart, M. *Chem. Mater*. **1991**, *3*, 805,

(15) Koc, R.; Kodambaka, S. K. *J. Eur. Ceram. Soc.* **2000**, *20*, 859.

(16) Koc, R.; Kodambaka, S. K. *J. Mater. Sci. Lett*. **1999**, *18*, 1469.

(17) Tan, G.-L.; Chen, C.-H.; Cheang, S.-C.; Uang, K.-M. *Appl. Phys. Lett*. **2004**, *85*, 2358.

(18) Mederios, F. F. P.; De Oliveira, S. A.; Desouza, C. P.; Da Sliva, A. G. P.; Gomes, U. U.; De souza, J. F. *Mater. Sci. Eng., A* **2001**, *315*, 58.

(19) Warren, A.; Bylund, A.; Ulefjord. I. *Int. J. Refract. Hard Met.* **1996**, *14*, 345.

(20) Girandon, J.-M.; Devassine, P.; Lamonier, J.-F.; Delannoy, L.; Lecleveq, L.; Leclereq, G. *J. Solid State Chem*. **2000**, *154*, 412.

(21) Ross, P. N.; Stonehart. P., Jr. *J. Catal.* **1975**, *39*, 789.

(22) Lee, K; Ishihara, A.; Mitsushima, S.; Kamiya, N.; Ota, K.-I. *Electrochim. Act.* **2004**, *49*, 3479.